Environmental Science & Technology

pubs.acs.org/est

Article

Community-Based Measurements Reveal Unseen Differences during Air Pollution Episodes

Kerry E. Kelly,*,# Wei W. Xing,# Tofigh Sayahi, Logan Mitchell, Tom Becnel, Pierre-Emmanuel Gaillardon, Miriah Meyer, and Ross T. Whitaker

Cite This: https://dx.doi.org/10.1021/acs.est.0c02341

Read Online

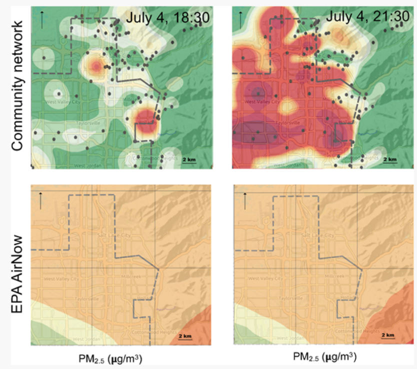

ABSTRACT: Short-term exposure to fine particulate matter ($PM_{2.5}$) pollution is linked to numerous adverse health effects. Pollution episodes, such as wildfires, can lead to substantial increases in $PM_{2.5}$ levels. However, sparse regulatory measurements provide an incomplete understanding of pollution gradients. Here, we demonstrate an infrastructure that integrates community-based measurements from a network of low-cost $PM_{2.5}$ sensors with rigorous calibration and a Gaussian process model to understand neighborhood-scale $PM_{2.5}$ concentrations during three pollution episodes (July 4, 2018, fireworks; July 5 and 6, 2018, wildfire; Jan 3−7, 2019, persistent cold air pool, PCAP). The firework/wildfire events included 118 sensors in 84 locations, while the PCAP event included 218 sensors in 138 locations. The model results accurately predict reference measurements during the fireworks (*n*: 16, hourly root-mean-square error, RMSE, 12.3−21.5 $\mu g/m^3$, n(normalized)-RMSE: 14.9−24%), the wildfire (*n*: 46, RMSE: 2.6−4.0 $\mu g/m^3$; nRMSE: 13.1−22.9%), and the PCAP (n: 96, RMSE: 4.9−5.7 $\mu g/m^3$; nRMSE: 20.2−21.3%). They also revealed dramatic geospatial differences in $PM_{2.5}$ concentrations that are not apparent when only considering government measurements or viewing the US Environmental Protection Agency's AirNow's visualizations. Complementing the $PM_{2.5}$ estimates and visualizations are highly resolved uncertainty maps. Together, these results illustrate the potential for low-cost sensor networks that combined with a data-fusion algorithm and appropriate calibration and training can dynamically and with improved accuracy estimate $PM_{2.5}$ concentrations during pollution episodes. These highly resolved uncertainty estimates can provide a much-needed strategy to communicate uncertainty to end users.

■ INTRODUCTION

Short- and long-term exposure to fine particulate matter ($PM_{2.5}$) pollution is linked to numerous adverse health effects,[1−3] and acute events, like wildfires and fireworks, can cause dramatic increases in $PM_{2.5}$ levels.[4,5] Although fewer studies have examined the health effects of $PM_{2.5}$ from these events, several studies suggest that wildfire smoke and fireworks cause adverse respiratory effects.[6,7] Pollution impacts from wildfires are becoming an increasing concern as both the number and size of wildfires continue to increase.[8] In fact, although air quality has improved in the US over the past 30 years, it has declined in wildfire-prone states.[9]

Conventionally, government organizations and researchers monitor ambient PM concentrations at sparsely distributed stations with advanced instrumentation. The high cost, labor, and maintenance requirements of these instruments result in measurements that are sparse in both space and time and that fail to capture localized $PM_{2.5}$ gradients within an urban area.[10,11] In addition, government organizations typically report hourly average PM concentrations at the conclusion of each hour. Both the sparse spatial distribution and the time lag in reporting results limit the ability of government monitoring stations to provide an early warning of a pollution event. Communities, researchers, and government organizations have deployed low-cost sensor networks in communities to collect more highly resolved air pollution data, e.g., throughout Taiwan,[12] Kansas City,[13] Oakland, CA,[14] and Memphis, TN,[15] for a variety of studies. These include identifying pollution hotspots and pollution sources,[15−17] understanding geospatial variability,[18] mapping air pollution with a dispersion model,[19] complementing land-use regression models,[20] and understanding smoke dispersion from prescribed fires.[21] However, these studies are generally short term, deploy fewer than 25 sensors (the studies in Taiwan and Oakland are exceptions[12,17]), and have not attempted to dynamically provide accurate and highly resolved pollution estimates coupled with visualizations. Furthermore, the results from these studies may not be easily accessible by the public.

Received: April 22, 2020
Revised: December 1, 2020
Accepted: December 2, 2020

Some organizations and researchers have begun publishing PM measurements from low-cost sensor networks.[22−24] However, if these sensor measurements are visualized, they are typically presented as colored dots on a map, with the colors typically corresponding to the US Environmental Protection Agency's (EPA) air quality index (AQI). Individuals can also view air-quality information on EPA's AirNow website as a heatmap,[25] but these maps are based on an interpolation of sparsely distributed government monitoring stations. Best practices for visualizing this information have not yet been developed.[26]

Here, we demonstrate an infrastructure, called AQ&U, that integrates community-hosted, low-cost, PM sensor network data from 84 locations, rigorous calibration strategies, data-fusion algorithms, and visualizations for understanding pollution events at a community level. These visualizations, in the form of maps, are available in near real time through a public-facing website.[27] In this study, we apply the AQ&U infrastructure to understand geospatial differences in $PM_{2.5}$ levels during two pollution episodes. This type of infrastructure is broadly applicable for dynamically understanding community-scale pollution gradients and offers numerous sustainability applications, such as congestion mitigation.

■ METHODS

This study focuses on three pollution events in Salt Lake City, UT, two during July 4−6, 2018, when the region experienced more than 10-fold increases in $PM_{2.5}$ levels from fireworks and the Dollar Ridge Wildfire. Maximum hourly $PM_{2.5}$ concentrations reached 116 and 75.4 $\mu g/m^3$ during the fireworks and the wildfire events, respectively (measured with federal equivalent methods, FEMs). The third event, a PCAP,[28] occurred during January 3−6, 2019, when $PM_{2.5}$ levels ranged from 0.4 to 63.5 $\mu g/m^3$. Table S1 and Figures S1−S8 show the $PM_{2.5}$ concentrations and meteorological conditions during the three events.

The $PM_{2.5}$ concentration measurements in the AQ&U infrastructure come from government sources—the Utah Division of Air Quality (DAQ)'s Sharp 5030i FEMs (2) monitors—and community-hosted sensors. The sharp FEMs use a combination of light-scattering nephelometry and β attenuation to measure $PM_{2.5}$ concentration. The community sensors provide measurements at 84 and 138 sites, respectively, for the firework/wildfire (F/WF) and PCAP events (Table S2). This yields an average sensor density of one node per 6.8 km^2 (F/WF) and 4.2 km^2 (PCAP), although the sensor density is not uniform as it is limited by the ability to identify willing sensor hosts with power and WiFi. The Plantower PMS sensor provides the PM measurements in the AirU (PMS3003) and the PurpleAir (PA) (PAI, PMS 1003 or PAII, PMS5003) nodes. The PA sensors and the PMS operating principles and performance are described elsewhere.[29,30] Briefly, the PMS sensors measure 90° light scattering with a photodetector that converts scattered laser light to $PM_{2.5}$ concentration, and the three different PMS models have slightly different internal configurations but use a similar laser wavelength and operating principle. The PMS $PM_{2.5}$ limit of detection (LOD) during summer is approximately 5 $\mu g/m^3$.[30] The AirU sensor is described in the study by Becnel et al.[31] It collects measurements every second, averages the data over 60 s, and transmits the measurements over the host's WiFi to an Influx database. The public can access sensor data from all sensor nodes through the AQ&U website or can download raw sensor data through an API.[27]

In addition to the AQ&U infrastructure, we use research-grade instrumentation mounted on a mobile platform for validation. These measurements are collected from the roof of TRAX light-rail train cars, which measure $PM_{2.5}$ concentrations with a Met One ES-642 nephelometer equipped with a $PM_{2.5}$ sharp-cut cyclone.[32] The TRAX train car is electrically powered and measures a variety of air pollutants and meteorological parameters.[32] The Met One ES-642 has a sampling frequency of 1 min and an instrument uncertainty of 1 $\mu g/m^3$. When this instrument was colocated with a DAQ FEM, it correlated reasonably well (R^2 = 0.74, RMSE = 4.13 $\mu g/m^3$, nRMSE = 89%, 8659 hourly measurements, Figure S9).[33]

Low-Cost Sensor Calibration. We apply both laboratory and field calibration to the AirU sensors and only field calibration to the PA sensors. The AirU PMS sensors are first calibrated in a laboratory chamber, which was characterized to have an error of less than 6% in $PM_{2.5}$ concentration.[34] The predeployment laboratory calibration aims to prevent the use of malfunctioning sensors and to understand intrasensor variability.[34] The AirU sensors were calibrated with aerosolized ammonium nitrate and alumina oxide over a concentration range of 5−150 $\mu g/m^3$ with a TSI DustTrak II using a $PM_{2.5}$ inlet, and they exhibited strong intrasensor agreement (R^2 > 0.97, 5-point calibration curve). Sensors were not deployed if during the laboratory calibration their linear relationship to the DustTrak had slopes that were not within 15% of the mean of all slopes or had intercepts not within 0 ± 4 $\mu g/m^3$. All of the AirU sensors in this study had spent fewer than 6 months in the field.

The raw $PM_{2.5}$ measurements from the AirU and PA sensor nodes are corrected using fits from colocated reference measurements for each event, fireworks, wildfire, or PCAP (Table S3,4). The corrected PMS sensor measurements (AirU and PA) correlated well with FEMs (fireworks: R^2 > 0.86 and RMSE < 11.3 $\mu g/m^3$; wildfire: R^2 > 0.91 and RMSE < 9.8 $\mu g/m^3$; PCAP: R^2 > 0.9 and RMSE < 5.8 $\mu g/m^3$). Clemens et al.[26] suggest that low-cost sensors correlating reasonably well with FEMs (R^2 = 0.4−0.8) can supplement existing monitoring networks to increase spatial coverage and fill knowledge gaps.

Data Screening. The raw low-cost sensor data set included 130 sensors in 87 locations for the F/WF and 218 sensors in 148 locations for the PCAP. The PAIIs contain two PMS5003 sensors per node. During the study period, we averaged the readings from the PAIIs if they agreed within 15% when the readings from the average of both sensors exceeded 5 $\mu g/m^3$. In addition, 5 sensors were removed for F/WF and 10 sensors were removed for the PCAP for exhibiting baseline drift, i.e., they never reached $PM_{2.5}$ levels below 15 $\mu g/m^3$ during the study period, although all other sensors in the data set did. Table S2 summarizes the number of sensors by type for each event before and after screening.

The TRAX $PM_{2.5}$ measurements were available at one-minute averages with corresponding GPS coordinates and instrument flow rates. Measurements associated with flow rates that were not within 10% of ES-642's design flow rate were excluded from the validation set (20% of measurements). TRAX travels in and out of the study domain, and we only used measurements that were inside of the study domain.

Data-Fusion Algorithm. An important goal of the AQ&U infrastructure is to provide dense, spatiotemporal estimates of

https://dx.doi.org/10.1021/acs.est.0c02341
Environ. Sci. Technol. XXXX, XXX, XXX−XXX

air quality and associated error estimates. For this, we use a Gaussian process (GP) model. GP models have two basic components. First, they assume that the sensor is corrupted by Gaussian noise and that the true signal ($PM_{2.5}$ concentrations in space−time) is a sample drawn from a Gaussian distribution with correlations between points that have a known form. Second, they are Bayesian, which means that GP models attempt to find a statistically formulated compromise between an estimate that approximately fits the noisy model that is likely, given the correlations that one would expect. In this way, space and time correlations are used to fuse measurements to offset the uncertainty of any one $PM_{2.5}$ measurement on its own.

For this work, based on our understanding of $PM_{2.5}$ sources, we choose a GP model where $PM_{2.5}$ concentrations have correlations that fall off monotonically with increased separation in time (t), space ($\mathbf{x}$), and altitude (a). In this paper, we use bold to denote a vector, and we denote a Gaussian/normal distribution as $G(\boldsymbol{\mu}, \sum)$, with mean $\boldsymbol{\mu}$ and covariance $\sum$. The sensor measurements are generated from a process, $y = f(\mathbf{x}, t) + \varepsilon$, where ε is independent, zero-mean, Gaussian noise, so that $\varepsilon \sim G(0, {\sigma_\varepsilon}^2)$, and σ_ε is estimated from the calibration of the sensors (RMSEs in Table S3). The function f has a probability described by a multivariate Gaussian distribution, $f \sim G(\boldsymbol{\mu}_f, \sum_f)$. We define the covariance of $\sum_f$ by specifying the pairwise correlations between $PM_{2.5}$ values at different times, locations, and altitudes. For this work, we make a standard simplification that these relationships are multiplicative:

$$c((\mathbf{x}, a, t), (\mathbf{x}', a', t')) = \theta_0 c_x(\mathbf{x}, \mathbf{x}')\, c_a(a, a')\, c_t(t, t') \tag{1}$$

where two different locations in space and time are denoted with and without a prime. The individual correlation functions fall off monotonically:

$$c_\alpha(\alpha, \alpha') = \exp\left(\frac{\|\alpha - \alpha'\|^2}{2\sigma_\alpha^2}\right) \text{ where } \alpha \in \{\mathbf{x}, a, t\} \tag{2}$$

where α will take the value of t, $\mathbf{x}$, and a (time, space, and attitude, respectively). Given this formulation of a prior, ($\boldsymbol{\mu}_f$, $\sum_f$) and a set of noisy measurements, the GP model performs a regression that gives $PM_{2.5}$ estimates at every point in space−time (altitude is a function of position, $a = a(x)$) that form a weighted average of nearby measurements with a smoothness prior that is introduced by the correlations in $\sum_f$. The construction of these estimates entails a linear algebraic solution (numerical matrix inversion).[35]

However, the GP formulation is not merely a regression but rather forms a probability function over the space of all possible $PM_{2.5}$ solutions. Because the assumptions are Gaussian, the resulting probabilities are Gaussian. For our $PM_{2.5}$ *estimate*, we use the mean of this distribution, which is also the mostly likely estimate (mode). However, because we have a full probability distribution over the space of solution, we also have a variance (and standard deviation) of the $PM_{2.5}$ estimates, which we present and visualize as *error* or *uncertainty* in this work.

The proposed model is general and makes some assumptions of smoothness, which are enforced through the correlation functions, c(). The degree of smoothness is expressed in the free parameters, the σ's, for each of the quantities (time, space, altitude), and the θ_0 term that controls the expected variation in $PM_{2.5}$ levels relative to the sensor. The parameters ($\sigma_x^2, \sigma_t^2, \sigma_{a,0}^2$) are learned from the input data using a maximum likelihood, cross-validation strategy. We optimize the parameters in these functions so that the resulting estimates best predict held out measurements, which properly accounts for sensor noise, helps establish a good level of smoothness in the regressed estimates, and avoids overfitting the sensor measurements.

In this data-driven estimation process, we observe that different air-quality events have distinct signal characteristics. For instance, $PM_{2.5}$ levels during PCAPs and wildfires tend to have stronger regularity in space and time, whereas the firework events change more rapidly and vary more across the area of study. Table S5 provides event-specific parameters. The uncertainty estimates also differ for the three events because the measurement errors differ for the three different events (Table S3 and S4).

Visualization. These results are translated into contours using standard plotting techniques from Matplotlib.[36] The visualization encodes the contours using a colormap based on the EPA AQI color scheme. This colormap divides each of the EPA AQI categories into three ranges, providing more resolved concentration information and differentiating it slightly from EPA's health-related color scheme, which is based on 24 h average pollutant concentrations.

RESULTS AND DISCUSSION

Gaussian Process Model Performance and Uncertainty Estimates. We evaluated Gaussian Process (GP) model predictions using a leave-one-out cross-validation at two Utah DAQ monitoring stations (Figures 1 and S10) and using mobile measurements collected from the TRAX light-rail system (Figure S11 and S12). This comparison of the GP model with the FEMs at the two DAQ monitoring stations (Hawthorne, HW, and Rose Park, RP) excluded the FEM measurements from the model input. Figures 1 and S10−12 illustrate that the GP model captures the $PM_{2.5}$ trends for both the fireworks, wildfire, and PCAP events. The root mean square errors (RMSEs) and normalized RMSEs (nRMSEs) of the hourly average model predictions compared to the corresponding FEM measurements were 12.3−21.5 μg/m^3 and 14.9−24.0% (fireworks, n = 16), 2.6−4.0 μg/m^3 and 13.1−22.9% (wildfire, n = 46), and 4.9−5.7 μg/m^3 and 20.2−21.3% (PCAP, n = 96), respectively. The GP model predictions correlate well with the TRAX measurements with an R^2 of 0.78 (F/WF) and 0.98 (PCAP), which is in the range of the TRAX instrumentation's correlation when colocated with the HW FEM (R^2 = 0.74, Figure S9).[33]

Figure 2 provides the uncertainty estimates for the study area during the three events. The measurement model has greater uncertainty for the firework event than the wildfire or PCAP events. These uncertainty differences can also be seen in Figure 1. The lowest uncertainty is associated with the highest sensor density in the central residential areas of Salt Lake City (<10, 4, or 6 μg/m^3 for fireworks, wildfire, and PCAP, respectively), while the highest uncertainty (<40, 14, or 23 μg/m^3 for fireworks, wildfire, and PCAP, respectively) is associated with the mountains on the east side of the city and the more industrial areas, including the airport, on the west side of the city for all events. Sensor siting is limited by the availability of power, WiFi, and a cooperative host. Consequently, the model estimates of $PM_{2.5}$ concentration in the mountains on the east

https://dx.doi.org/10.1021/acs.est.0c02341
Environ. Sci. Technol. XXXX, XXX, XXX−XXX

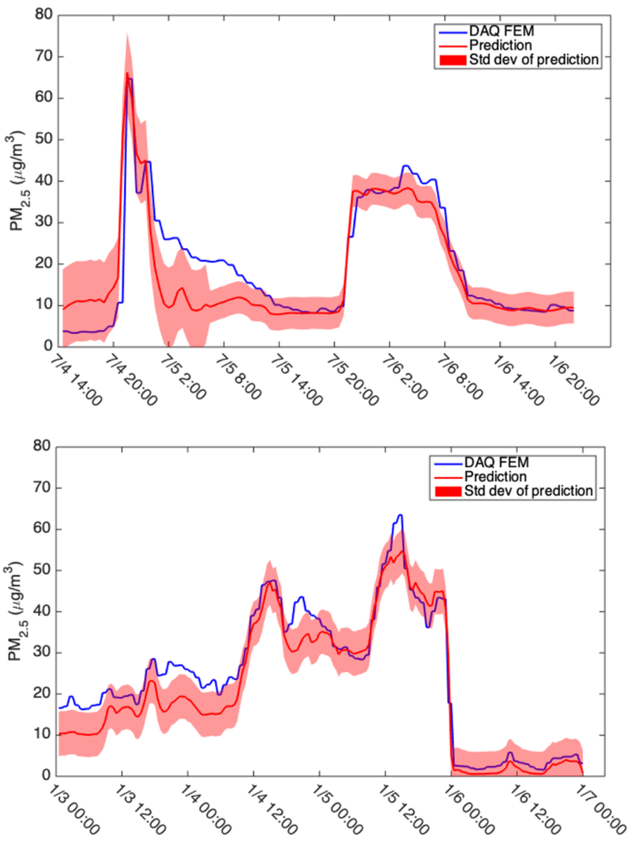

Figure 1. Comparison of DAQ FEM $PM_{2.5}$ measurements with the GP model predictions at the Hawthorne monitoring stations during the F/WF event (top) and the PCAP event (bottom). The FEM measurements were excluded from the model for these predictions. The FEM measurements are hourly averages, while the GP model predictions are every 15 min.

side of the Salt Lake Valley should be considered in light of the high uncertainty.

The model performs best during all events in areas with high sensor density, approximately 1 sensor per 3 km^2. For example, the RMSEs of the model predictions compared to the FEMs are within the ranges reported by studies that compare the field performance of low-cost PM sensors to nearby reference instrumentation (hourly average: 3.89−13.1 $\mu g/m^3$ PMS5003,[37] 6.8 $\mu g/m^3$ PMS7003,[38] 10.6 $\mu g/m^3$ PMS5003,[39] 14.7 $\mu g/m^3$ Alphasense OPC-N2,[38] 27−31 $\mu g/m^3$ PMS 3003[40]). However, the model does not perform as well at the RP station during the F/WF events (Figure S10). It underpredicts $PM_{2.5}$ concentrations at the RP station during periods of elevated windspeed (Figures S2,3). This underprediction is likely due to the presence of windblown dust from the north and east of the RP station, which is located approximately 5 km southeast of the dry lakebed surrounding the Great Salt Lake and 3 km west of a gravel pit. Consequently, the presence of confounding factors, such as windblown dust, should be considered when interpreting the sensor data and model results. The low-cost sensors used in the AQ&U infrastructure (PMS 1003, 3003, and 5003) are inefficient at measuring windblown dust and coarser fractions of PM.[30,41,42] The GP model also overpredicts the peak $PM_{2.5}$ concentration at the RP station during the firework event, perhaps because of the variable particle size distribution and spatially heterogeneous nature of fireworks.[42] However, the model still captures the general $PM_{2.5}$ trends, and the nRMSE of less than 24% is in the range reported for calibrated PMS sensors in previous studies (23−50%).[39,43]

The model predictions agree with the trends shown by the TRAX measurements during all events, although they suggest higher $PM_{2.5}$ levels than TRAX (Figure S11,12). Because many of the TRAX measurements were made while the train was moving through the domain, we do not necessarily expect a perfect correlation during the events. In addition, the Met One nephelometer estimates $PM_{2.5}$ concentration optically. These types of optical measurements require a particle-specific correction factor to convert light scattering to particle mass concentration,[44] although this information was not available.

Firework Event. Figure 3a−c illustrates the large temporal differences in $PM_{2.5}$ levels in the Salt Lake Valley during the July 4th holiday. Before the fireworks begin at 6 pm, $PM_{2.5}$ levels were 8.1−8.2 $\mu g/m^3$, but levels rapidly increase at 8 pm and reach a maximum of 64.7 and 116 $\mu g/m^3$ at the two state monitoring stations (located 8.5 km apart). By 1 am on July 5th, $PM_{2.5}$ levels decline. The DAQ and EPA define the hourly $PM_{2.5}$ average concentration for an hour, say 8 pm, as the average over 8:00 to 8:59 pm. These short-term spikes in $PM_{2.5}$ concentrations associated with fireworks are common during the 4th of July independence holiday in the US. In fact, another Utah monitoring station reported an hourly average $PM_{2.5}$ concentration of 900 $\mu g/m^3$ during a firework event.[45] Figure 3a−c also illustrates large geospatial differences, which are likely due to the region's fireworks policy. Because of the extreme fire danger in this arid region, local officials prohibit fireworks near the urban-wildland interface (dotted line in Figure 3). The GP model estimates $PM_{2.5}$ concentrations

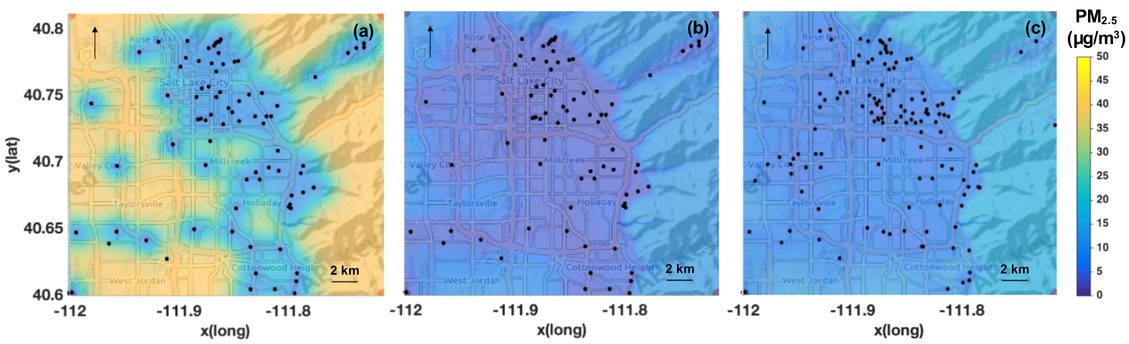

Figure 2. Uncertainty estimates from the GP model for the (a) fireworks, (b) wildfire (b), and (c) PCAP events. The dots denote sensor locations. Some sensor locations are hidden at the request of the hosts.

https://dx.doi.org/10.1021/acs.est.0c02341
Environ. Sci. Technol. XXXX, XXX, XXX−XXX

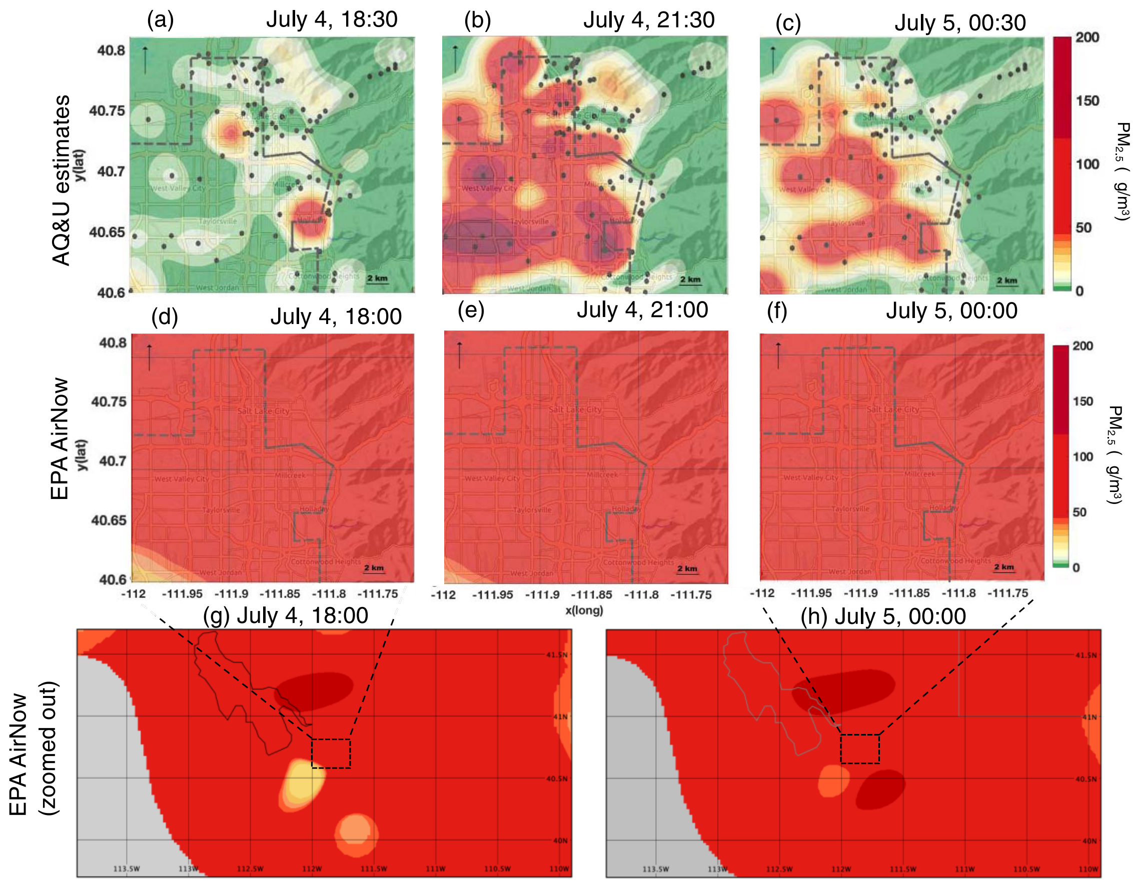

Figure 3. Time series of $PM_{2.5}$ concentrations from the GP-sensor model (panel a−c) and the EPA AirNow estimates of $PM_{2.5}$ concentration (panel d−h) in the Salt Lake Valley on July 4, 2018. The dots in panels a to c denote sensor locations although some dots are not shown at the request of the host. Fireworks are allowed in the southwest portion of the study area, and the dotted line in panels a through f designates the boundary where fireworks are prohibited. Panels g and h are zoomed-out images from AirNow with the box indicating the study area.

within the firework zone at 81.3 $\mu g/m^3$ between 9 and 10 pm, while they average 12.5 $\mu g/m^3$ in the restricted area (Table S6). Considering only the sensors, $PM_{2.5}$ concentrations average 92.0 and 7.9 $\mu g/m^3$ inside and outside of the firework zone, respectively. This difference is statistically significant (Student's t-test, $p < 0.001$). Both the GP model predictions and the sensor measurements confirm the effect of the firework restriction. The differences between the sensor measurements and the GP model estimates are likely due to the uneven geospatial distribution of the sensors.

Wind contributed to the geospatial differences in $PM_{2.5}$ concentration during the firework event. Between 8 and 11 pm, winds were light at 4.3 km/h and predominantly from the east (Figures S2,3). During this time of day, thermally driven flows exit the canyons on the east side of the valley,[46] and these flows tend to prevent the transport of the firework emissions to the east. In this city, $PM_{2.5}$ levels also tend to be higher at the lower elevations, where the major roads are located;[47] however, these geospatial concentration differences are much greater during the firework event than before or after.

The US EPA generates publicly available hourly $PM_{2.5}$ estimates and visualizations. Figure 3d−h shows the AirNow $PM_{2.5}$ estimates for selected time periods and that correspond to the GP model predictions. Figure 3 shows the GP model predictions for the middle of each hour, while the AirNow estimates are for the hourly average $PM_{2.5}$ concentration. Figure S13 shows the same results, but with AirNow concentrations at a more finely resolved scale. The EPA uses an inverse distance weighting approach to interpolate air quality measures from government monitoring stations. This interpolation ignores topographic features, and the GP model predictions and FEM measurements suggest that using inverse distance weighting with sparsely distributed measurements can lead to inaccurate estimates of $PM_{2.5}$ concentrations in the complex terrain of the Salt Lake Valley. For example, in the Salt Lake Valley, for the 6 pm hour on July 4, $PM_{2.5}$ sensor measurements throughout the study area average 7.0 $\mu g/m^3$ (8.1−8.2 $\mu g/m^3$, HW and RP, respectively). However, the AirNow estimates show $PM_{2.5}$ concentrations in the range of 58−68 $\mu g/m^3$ for the majority of the study areas during this same time period. These elevated AirNow estimates are likely due to regional wildfire activity and can be more clearly seen as the AirNow visualizations zoom out (Figures 3 and S13g,h).[48−50] As another example, at the peak of firework activity (9 pm hour on July 4), AirNow does not capture the geospatial differences associated with the fireworks and shows $PM_{2.5}$ concentrations ranging from 28 to 68 $\mu g/m^3$ for the entire study area, while the model shows an average of 81.3 $\mu g/m^3$ within the firework area and 4-fold lower levels outside of the firework zones. AirNow also shows the lowest $PM_{2.5}$ concentrations in the southeast quadrant of the study area, which disagrees with the sensor and model estimates as well as the TRAX measurements. Table S6 provides the summary statistics that correspond to Figure 3.

https://dx.doi.org/10.1021/acs.est.0c02341
Environ. Sci. Technol. XXXX, XXX, XXX−XXX

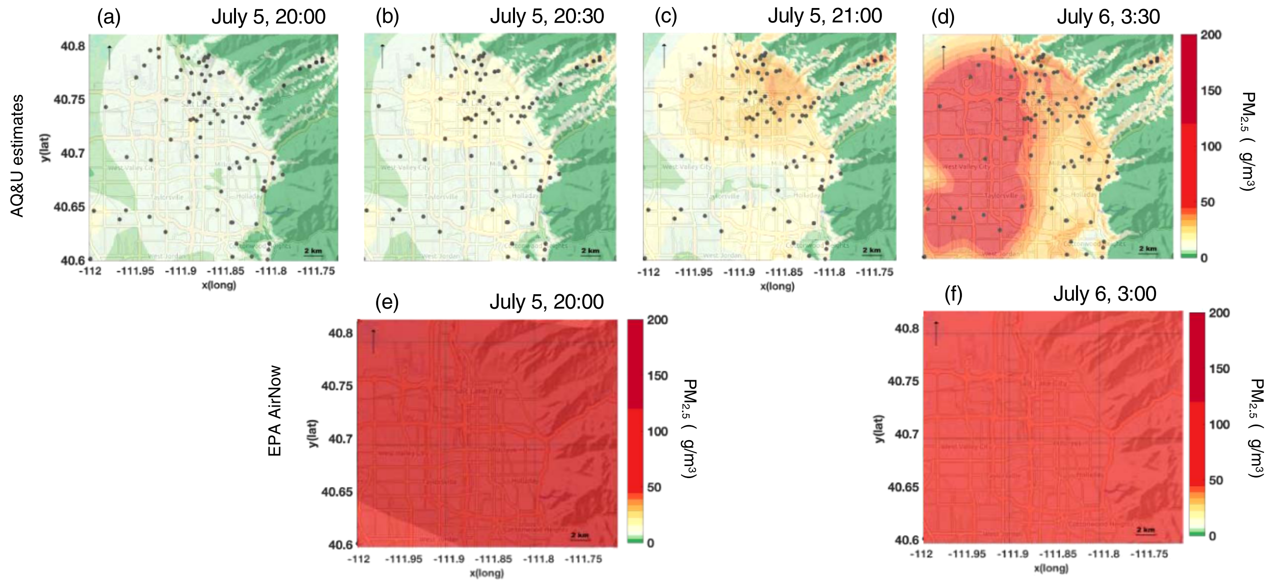

Figure 4. Time series of $PM_{2.5}$ concentration estimates for July 5 and 6, 2018, when Salt Lake City experienced smoke from the Dollar Ridge wildfire. Panels a−d show the GP model predictions, and panels e and f show the EPA AirNow estimates for the study area. The dots in panels a−c denote sensor locations, although some dots are not shown at the request of the host. See Figure S14 for higher-resolution AirNow estimates.

Wildfire Event. Figure 4 and S14 demonstrate another case in which the low-cost sensor network and GP model can complement regulatory measurements. On July 5, 2018, smoke from the 69 000-acre Dollar Ridge Fire began to affect Salt Lake City.[48−50] Between 8 and 9 pm (Figure 4a), the five AQ&U network sensors on the east side of the valley show more than a 3-fold increase in $PM_{2.5}$ concentrations (from 7.2 to 29.4 $\mu g/m^3$). Between 9 and 10 pm, the $PM_{2.5}$ concentrations at the state monitoring stations increase 3-fold from 8.8 to 26.9 $\mu g/m^3$ (average of two FEMs, Figure S15). The state does not report the 9 to 9:59 pm measurements until approximately 10:30 pm. Consequently, at least 1.5 h elapse between the time when the AQ&U network sensors begin to show an increase and when the state monitoring stations report this increase. Because of the relatively high uncertainty in the mountains on the east side of the Salt Lake Valley (<20 $\mu g/m^3$, Figure 2), it is difficult to determine whether the plume is flowing down the canyon or over the tops of the mountains.

The large spatial and temporal variations in $PM_{2.5}$ levels have been reported for other fire events. Kelleher et al.[21] observed strong temporal and spatial concentration gradients associated with a wildfire in complex terrain using a network of 13 Sharp GP2Y1023AU0F PM sensors. They mapped 24 h average $PM_{2.5}$ levels from prescribed fire in southern Colorado using ordinary Kriging, one example of a GP model. However, the infrastructure we demonstrate allows much finer spatial and temporal resolution and offers the opportunity to provide estimates in near real time.

PCAP Event. Figures 1 and S16 illustrate the temporal and spatial differences in $PM_{2.5}$ concentration during a PCAP event. They show that GP model predictions of $PM_{2.5}$ concentrations increase as the PCAP builds and then decrease rapidly on January 6, 2019, tracking the FEM measurements. Figure S16 demonstrates how $PM_{2.5}$ concentrations decrease with increasing elevation during the PCAP, as reported in previous studies.[28] Figure 1 also suggests that the GP model performs reasonably well for the low levels of $PM_{2.5}$ (~5 $\mu g/m^3$) on January 6, 2020 (RMSE: 1.5−4.8 $\mu g/m^3$, nRMSE: 47.3−89.5%, n: 24). During this entire event, AirNow fails to capture the geospatial variations associated with the complex terrain of this region.

Difference between Events. The geospatial patterns in $PM_{2.5}$ concentration differed during the three events. Figures S17−S22 show the coefficients of determination between the sensor measurements and the two FEMs versus distance and elevation. During the firework event, the sensor measurements were not well correlated with the FEMs, suggesting the spatial heterogeneity of the firework event as well as potentially time-varying size distributions during this event (Figures S17 and S18, more than half of the measurements exhibiting R^2 values < 0.7). Figure 3 and the GP-model-specific parameters (Table S5) also support the spatial heterogeneity of firework-associated $PM_{2.5}$ concentrations. In addition, the sensors at the highest elevations were uncorrelated with the FEMs (Figure S18), supporting the effectiveness of the firework restrictions. In contrast, PM levels during the wildfire event were affected by regional wildfires, and although concentration gradients existed, the PM measurements were well correlated with the FEMs (Figure 4, S19, and S20, more than half of the measurements exhibited R^2 values > 0.7). During the PCAP event, $PM_{2.5}$ was strongly correlated with elevation with 90% of sensors located within 100 m of elevation of the FEMs having R^2 > 0.7 (Figure S21). This elevation-dependent behavior of $PM_{2.5}$ is consistent with previous studies of PCAPs in this region.[51,52]

Obtaining Highly Resolved Estimates of Air Quality. Other studies have employed land use regression (LUR) methods to estimate more highly resolved air-pollutant concentrations in regions with sparse measurements. LURs typically require the collection of substantial amounts of geographic information and significant measurement campaigns. More recently, mobile and low-cost measurements have been used to improve LUR models.[20,53−55] The problem researchers address with LURs is different than the one we address here. They generally use LURs to predict air quality for a long time period, i.e., a season, in the absence of direct measurements, whereas the sensor network described here presents the opportunity to directly measure acute events, with the challenge of how to best integrate the broad set of spatiotemporal data from a low-cost sensor network.

This study used a GP model to predict $PM_{2.5}$ concentrations from a dense network of community-hosted sensors. This is one example of how citizen science can complement government and research measurements to improve the spatial extent and resolution of pollution estimates.[56] Our results demonstrate the value of low-cost sensor networks coupled with a validated GP model for resolving fine spatial gradients during pollution episodes, particularly when compared to the EPA's AirNow visualizations that interpolate sparse measurements across complex terrain. Li et al.[57] also highlight the challenge of complex terrain when developing PM concentration estimates. In another example, a study mapped $PM_{2.5}$ levels associated with fireworks in the Salt Lake Valley using only state reference and TRAX measurements with inverse distance weighting.[33] However, this study could not resolve the geospatial detail away from the measurement locations, such as the effect of firework restrictions, presented here.

The results highlighted in this paper have limitations, several of which are currently active areas of research, and some practical considerations need to be addressed before this type of framework could be deployed to dynamically provide pollution estimates in a community. First, this framework requires supervision to generate high-quality results. For example, the model parameters need to be developed for each season and each event (i.e., Table S5). A more efficient strategy is needed. Quality control and data screening need to become more automated and systematic.[58−60] Second, the framework could become more robust through studying additional conditions. Third, the development of appropriate correction factors relies on elevated $PM_{2.5}$ levels, and aerosol properties can vary dramatically event by event, leading to the need for event-specific correction factors. In our experience, the PMS sensor responses tend to be relatively consistent for PCAP events and the winter season as a whole (Figure S30,31).[30] However, during seasons with a variety of events, such as summer with fireworks, wildfires, and dust storms, the correction factors can vary by more than a factor of 4, which, in turn, could lead to highly inaccurate results if the incorrect correction factor is selected. Fourth, the measurements also rely on citizen hosted data, and the results do not consider siting impacts, although previous studies suggest little sensitivity associated with siting impacts.[61] Fifth, the sensor distribution is not optimal, in part because some areas of the study domain lack suitable infrastructure (i.e., power, WiFi, and hosts) so the uncertainty in some of these locations is relatively high. However, the areas with the highest areas of uncertainty are either sparsely populated or located in industrial areas.

In spite of the limitations, this study demonstrates the potential for low-cost sensor networks that combined with a data-fusion algorithm and appropriate calibration and training can dynamically and with improved accuracy estimate $PM_{2.5}$ concentrations during pollution episodes. These highly resolved $PM_{2.5}$ and uncertainty estimates can be rapidly visualized and communicated to a community. The validation results, including coefficients of determination, RMSEs, and nRMSEs compared to FEMs, suggest that the data from low-cost sensor networks can complement regulatory measurements to reveal important differences in air quality. Here, we demonstrate the ability to capture 4-fold differences in $PM_{2.5}$ levels associated with firework restrictions that are not evident from the DAQ sites or EPA AirNow's visualizations. We also identify an approaching smoke plume at least 1.5 h before it is reported by the DAQ and strong elevation trends in $PM_{2.5}$ during a PCAP. The visualizations address the challenge of having individuals interpolate their results for themselves (i.e., from colored dots on a map), and the complementary uncertainty maps contribute to the development of much-needed strategies to integrate and communicate information from low-cost sensing networks. Taken together, this type of infrastructure that leverages citizen science allows the community to more clearly understand the fine-graded differences in pollution concentration, which is particularly important in regions with complex terrain. Ultimately, this type of approach could be integrated with government-sponsored public information to provide more timely and geospatially accurate air-quality alerts.

■ ASSOCIATED CONTENT

Supporting Information

The Supporting Information is available free of charge at https://pubs.acs.org/doi/10.1021/acs.est.0c02341.

> Meteorological information; wind roses; comparison of TRAX measurements to FEM; comparison of GP model estimates to FEM and TRAX measurements; comparison of GP model estimates to EPA AirNow visualizations; relationships between the sensor distance and elevation, and FEM measurements; calibration relationships between sensors and FEMs; scatterplots of the calibration relationships; sensors included in GP model estimates; and GP model parameters (PDF)

■ AUTHOR INFORMATION

Corresponding Author

Kerry E. Kelly − *Department of Chemical Engineering, University of Utah, Salt Lake City, Utah 84112, United States;* orcid.org/0000-0002-2232-3092; Email: kerry.kelly@utah.edu

Authors

Wei W. Xing − *Scientific Computing and Imaging Institute, University of Utah, Salt Lake City, Utah 84112, United States*

Tofigh Sayahi − *Department of Chemical Engineering, University of Utah, Salt Lake City, Utah 84112, United States*

Logan Mitchell − *Department of Atmospheric Sciences, University of Utah, Salt Lake City, Utah 84112, United States;* orcid.org/0000-0002-8749-954X

Tom Becnel − *School of Computing, University of Utah, Salt Lake City, Utah 84112, United States*

Pierre-Emmanuel Gaillardon − *School of Computing, University of Utah, Salt Lake City, Utah 84112, United States*

Miriah Meyer − *Department of Electrical and Computer Engineering, University of Utah, Salt Lake City, Utah 84112, United States*

Ross T. Whitaker − *Department of Electrical and Computer Engineering, University of Utah, Salt Lake City, Utah 84112, United States*

Complete contact information is available at: https://pubs.acs.org/10.1021/acs.est.0c02341

https://dx.doi.org/10.1021/acs.est.0c02341
Environ. Sci. Technol. XXXX, XXX, XXX−XXX

Author Contributions

[#]K.E.K. and W.W.X. contributed equally to this work.

Notes

The authors declare the following competing financial interest(s): Dr. Kerry Kelly and Dr. Gaillardon have financial interest in the company Tetrad: Sensor Network Solutions, LCC, which commercializes solutions for environmental monitoring.

■ ACKNOWLEDGMENTS

The authors gratefully acknowledge NSF support by CPS: Synergy: A Layered Framework of Sensors, Models, Land-Use Information and Citizens for Understanding Air Quality in Urban Environments (1646408), and EAGER: AirU: Community Network to Understand Air Quality and Sensor Reliability (1642513). We are also grateful for support from the Lawrence T. and Janet T. Dee Foundation as well as UCAIR. Thanks to PurpleAir for sharing their data and to the Utah Division of Air Quality for allowing colocation of low-cost sensors at their monitoring station. Thanks to Ethan Brown (US EPA Region 8) who provided the historical AirNow data.

■ REFERENCES

(1) *State of Global Air 2018*; HEI: Boston, MA, 2018.

(2) Lin, H.; Ratnapradipa, K.; Wang, X.; Zhang, Y.; Xu, Y.; Yao, Z.; Dong, G.; Liu, T.; Clark, J.; Dick, R.; Xiao, J.; Zeng, W.; Li, X.; Qian, Z.; Ma, W. Hourly peak concentration measuring the PM2.5-mortality association: Results from six cities in the Pearl River Delta study. *Atmos. Environ.* **2017**, *161*, 27−33.

(3) Liang, F.; Xiao, Q.; Gu, D.; Xu, M.; Tian, L.; Guo, Q.; Wu, Z.; Pan, X.; Liu, Y. Satellite-based short- and long-term exposure to PM2.5 and adult mortality in urban Beijing, China. *Environ. Pollut.* **2018**, *242*, 492−499.

(4) Seidel, D. J.; Birnbaum, A. N. Effects of Independence Day fireworks on atmospheric concentrations of fine particulate matter in the United States. *Atmos. Environ.* **2015**, *115*, 192−198.

(5) Crippa, P.; Castruccio, S.; Archer-Nicholls, S.; Lebron, G. B.; Kuwata, M.; Thota, A.; Sumin, S.; Butt, E.; Wiedinmyer, C.; Spracklen, D. V. Population exposure to hazardous air quality due to the 2015 fires in Equatorial Asia. *Sci. Rep.* **2016**, *6*, No. 37074.

(6) Navarro, K.; Schweizer, D.; Balmes, J.; Cisneros, R. A Review of Community Smoke Exposure from Wildfire Compared to Prescribed Fire in the United States. *Atmosphere.* **2018**, *9*, No. 185.

(7) Gouder, C.; Montefort, S. Potential impact of fireworks on respiratory health. *Lung India* **2014**, *31*, 375−379.

(8) Jolly, W. M.; Cochrane, M. A.; Freeborn, P. H.; Holden, Z. A.; Brown, T. J.; Williamson, G. J.; Bowman, D. M. J. S. Climate-induced variations in global wildfire danger from 1979 to 2013. *Nat. Commun.* **2015**, *6*, No. 7537.

(9) McClure, C. D.; Jaffe, D. A. US particulate matter air quality improves except in wildfire-prone areas. *Proc. Natl. Acad. Sci. U.S.A.* **2018**, *115*, 7901−7906.

(10) Steinle, S.; Reis, S.; Sabel, C. E. Quantifying human exposure to air pollution–moving from static monitoring to spatio-temporally resolved personal exposure assessment. *Sci. Total Environ.* **2013**, *443*, 184−193.

(11) Apte, J. S.; Messier, K. P.; Gani, S.; Brauer, M.; Kirchstetter, T. W.; Lunden, M. M.; Marshall, J. D.; Portier, C. J.; Vermeulen, R. C. H.; Hamburg, S. P. High-Resolution Air Pollution Mapping with Google Street View Cars: Exploiting Big Data. *Environ. Sci. Technol.* **2017**, *51*, 6999−7008.

(12) Lin, Y.-C.; Chi, W.-J.; Lin, Y.-Q. The improvement of spatial-temporal resolution of PM2.5 estimation based on micro-air quality sensors by using data fusion technique. *Environ. Int.* **2020**, *134*, No. 105305.

(13) Kimbrough, S.; Krabbe, S.; Baldauf, R.; Barzyk, T.; Brown, M.; Brown, S.; Croghan, C.; Davis, M.; Deshmukh, P.; Duvall, R.; Feinberg, S.; Isakov, V.; Logan, R.; McArthur, T.; Shields, A. The Kansas City transportation and local-scale air quality study (KC-TRAQS): Integration of low-cost sensors and reference grade monitoring in a complex metropolitan area. Part 1: Overview of the project. *Chemosensors* **2019**, *7*, No. 26.

(14) English, P. B.; Olmedo, L.; Bejarano, E.; Lugo, H.; Murillo, E.; Seto, E.; Wong, M.; King, G.; Wilkie, A.; Meltzer, D.; Carvlin, G.; Jarrett, M.; Northcross, A. The Imperial County Community Air Monitoring Network: A Model for Community-based Environmental Monitoring for Public Health Action. *Environ. Health Perspect.* **2017**, *125*, 74501.

(15) Feinberg, S. N.; Williams, R.; Hagler, G.; Low, J.; Smith, L.; Brown, R.; Garver, D.; Davis, M.; Morton, M.; Schaefer, J.; Campbell, J. Examining spatiotemporal variability of urban particulate matter and application of high-time resolution data from a network of low-cost air pollution sensors. *Atmos. Environ.* **2019**, *213*, 579−584.

(16) Gao, M.; Cao, J.; Seto, E. A distributed network of low-cost continuous reading sensors to measure spatiotemporal variations of PM2.5 in Xi'an, China. *Environ. Pollut.* **2015**, *199*, 56−65.

(17) Caubel, J. J.; Cados, T. E.; Preble, C. V.; Kirchstetter, T. W. A Distributed Network of 100 black carbon sensors for 100 Days of air quality monitoring in West Oakland, California. *Environ. Sci. Technol.* **2019**, *53*, 7564−7573.

(18) Shafran-Nathan, R.; Etzion, Y.; Zivan, O.; Broday, D. M. Estimating the spatial variability of fine particles at the neighborhood scale using a distributed network of particle sensors. *Atmos. Environ.* **2019**, *218*, No. 117011.

(19) Schneider, P.; Castell, N.; Vogt, M.; Dauge, F. R.; Lahoz, W. A.; Bartonova, A. Mapping urban air quality in near real-time using observations from low- cost sensors and model information. *Environ. Int.* **2017**, *106*, 234−247.

(20) Masiol, M.; Zíková, N.; Chalupa, D. C.; Rich, D. Q.; Ferro, A. R.; Hopke, P. K. Hourly land-use regression models based on low-cost PM monitor data. *Environ. Res.* **2018**, *167*, 7−14.

(21) Kelleher, S.; Quinn, C.; Miller-Lionberg, D.; Volckens, J. A low-cost particulate matter (PM2.5) monitor for wildland fire smoke. *Atmos. Meas. Tech.* **2018**, *11*, 1087−1097.

(22) Jiao, W.; Hagler, G.; Williams, R.; Sharpe, R.; Brown, R.; Garver, D.; Judge, R.; Caudill, M.; Rickard, J.; Davis, M.; Weinstock, L.; Zimmer-Dauphinee, S.; Buckey, K. Community Air Sensor Network (CAIRSENSE) project: Evaluation of low-cost sensor performance in a suburban environment in the southeastern United States. *Atmos. Meas. Tech.* **2016**, *9*, 5281−5292.

(23) PurpleAir. PurpleAir Air Quality Map, http://map.purpleair.org/. Accessed Oct 02, 2016.

(24) IVAN: Imperial Valley Air Quality Monitoring Network, https://www.ivan-imperial.org/air/map. 2020.

(25) US-EPA. AirNow. https://airnow.gov/.

(26) Clements, A. L.; Griswold, W. G.; RS, A.; Johnston, J. E.; Herting, M. M.; Thorson, J.; Collier-Oxandale, A.; Hannigan, M. Low-cost air quality monitoring tools: From Research to Practice (A Workshop Summary). *Sensors* **2017**, *17*, 2478.

(27) AQ&U. 2020, aqandu.org.

(28) Whiteman, C. D.; Hoch, S. W.; Horel, J. D.; Charland, A. Relationship between particulate air pollution and meteorological variables in Utah's Salt Lake Valley. *Atmos. Environ.* **2014**, *94*, 742−753.

(29) Kelly, K. E.; Whitaker, J.; Petty, A.; Widmer, C.; Dybwad, A.; Sleeth, D.; Martin, R.; Butterfield, A. Ambient and laboratory evaluation of a low-cost particulate matter sensor. *Environ. Pollut.* **2017**, *221*, 491−500.

(30) Sayahi, T.; Butterfield, A. E.; Kelly, K. E. Long-term field evaluation of the Plantower PMS low-cost particulate matter sensors. *Environ. Pollut.* **2019**, *245*, 932−940.

(31) Becnel, T.; Sayahi, T.; Le, K.; Goffin, P.; Butterfield, T.; Kelly, K.; Gaillardon, P.-E. A distributed low-cost pollution monitoring platform. *Internet Things J.* **2019**, *6*, 10738−10748.

(32) Mitchell, L. E.; Crosman, E. T.; Jacques, A. A.; Fasoli, B.; Leclair-Marzolf, L.; Horel, J.; Bowling, D. R.; Ehleringer, J. R.; Lin, J. C. Monitoring of greenhouse gases and pollutants across an urban area using a light-rail public transit platform. *Atmos. Environ.* **2018**, *187*, 9−23.

(33) Mendoza, D. L.; Crosman, E. T.; Mitchell, L. E.; Jacques, A. A.; Fasoli, B.; Park, A. M.; Lin, J. C.; Horel, J. D. The TRAX Light-rail train air quality observation Project. *Urban Sci.* **2019**, *3*, 108.

(34) Sayahi, T.; Kaufman, D.; Becnel, T.; Kaur, K.; Butterfield, A. E.; Collingwood, S.; Zhang, Y.; Gaillardon, P.-E.; Kelly, K. E. Development of a calibration chamber to evaluate the performance of low-cost particulate matter sensors. *Environ. Pollut.* **2019**, *255*, No. 113131.

(35) Rasmussen, C. E.; Williams, C. K. I. *Gaussian Processes for Machine Learning*; MIT Press: Cambridge, MA, 2006.

(36) Padilla, L.; Quinan, P. S.; Meyer, M.; Creem-Regehr, S. H. Evaluating the impact of binning 2D scalar fields. *IEEE Trans. Vis. Comput. Graphics* **2017**, *23*, 431−440.

(37) Ardon-Dryer, K.; Dryer, Y.; Williams, J. N.; Moghimi, N. Measurements of PM2.5 with PurpleAir under atmospheric conditions. *Atmos. Meas. Tech. Discuss.* **2019**, *2019*, 5441−5458.

(38) Bulot, F. M. J.; Johnston, S. J.; Basford, P. J.; Easton, N. H. C.; Apetroaie-Cristea, M.; Foster, G. L.; Morris, A. K. R.; Cox, S. J.; Loxham, M. Long-term field comparison of multiple low-cost particulate matter sensors in an outdoor urban environment. *Sci. Rep.* **2019**, *9*, No. 7497.

(39) Si, M.; Xiong, Y.; Du, S.; Du, K. Evaluation and calibration of a low-cost particle sensor in ambient conditions using machine learning technologies. *Atmos. Meas. Tech. Discuss.* **2020**, *13*, 1693−1707.

(40) Zheng, T.; Bergin, M. H.; Johnson, K. K.; Tripathi, S. N.; Shirodkar, S.; Landis, M. S.; Sutaria, R.; Carlson, D. E. Field evaluation of low-cost particulate matter sensors in high- and low-concentration environments. *Atmos. Meas. Tech.* **2018**, *11*, 4823−4846.

(41) Zhu, L.; Jacob, D. J.; Keutsch, F. N.; Mickley, L. J.; Sche, R.; Strum, M.; Gonza, G.; Chance, K.; Yang, K.; Rappengluck, B.; Millet, D. B.; Baasandorj, M.; Jaegle, L.; Shah, V. Formaldehyde (HCHO) as a hazardous air pollutant: mapping surface air concentrations from satellite and inferring cancer risks in the United States. *Environ. Sci. Technol.* **2017**, *51*, 5650−5657.

(42) Kuula, J.; Mäkelä, T.; Aurela, M.; Teinilä, K.; Varjonen, S.; Gonzales, O.; Timonen, H. Laboratory evaluation of particle size-selectivity of optical low-cost particulate matter sensors. *Atmos. Meas. Tech. Discuss.* **2019**, *2019*, 1−21.

(43) Zheng, T.; Bergin, M. H.; Johnson, K. K.; Tripathi, S. N.; Shirodkar, S.; Landis, M. S.; Sutaria, R.; Carlson, D. E. Field evaluation of low-cost particulate matter sensors in high- and low-concentration environments. *Atmos. Meas. Tech.* **2018**, 4823−4846.

(44) Dacunto, P. J.; Klepeis, N. E.; Cheng, K.-C.; Acevedo-Bolton, V.; Jiang, R.-T.; Repace, J. L.; Ott, W. R.; Hildemann, L. M. Determining PM2.5 calibration curves for a low-cost particle monitor: common indoor residential aerosols. *Environ. Sci. Process. Impacts* **2015**, *17*, 1959−1966.

(45) Yu, Y.-S. *The Pollution Problem of Utah's July Fireworks — When the 'Oohs' and 'Aahs' Turn to 'Ewws' and 'Ughs*; Salt Lake Tribune: Salt Lake City, 2019.

(46) Zardi, D.; Whiteman, C. D. Diurnal mountain wind systems, In *Mountain Weather Research and Forecasting*, Chow, F. K.; DeWekker, S. F. J.; Snyder, B., Eds.; Springer Verlag: 2012; pp 35−119.

(47) Mullen, C.; Grineski, S.; Collins, T.; Xing, W.; Whitaker, R.; Sayahi, T.; Becnel, T.; Goffin, P.; Gaillardon, P.-E.; Kelly, K. Patterns of distributive environmental inequity under different PM2.5 air pollution scenarios for Salt Lake County public schools (in revision). *Environ. Res.* **2020**, No. 109543.

(48) Dollar Ridge Fire Update - July 2, https://utahfireinfobox.com/2018/07/02/dollar-ridge-fire-update-july-2/. 2020.

(49) Dollar Ridge Fire, https://en.wikipedia.org/wiki/Dollar_Ridge_Fire. Accessed Feb 11, 2020.

(50) Maffley, B. *It Smells Like Fire, And The Haze is Thick. The Salt Lake Valley's Air Faces a "Double'whammy" from Fires and Ozone*; Salt Lake Tribuneake Tribune: Salt Lake City, UT, 2018.

(51) Silcox, G. D.; Kelly, K. E.; Crosman, E. T.; Whiteman, C. D.; Allen, B. L. Wintertime PM2.5 concentrations during persistent, multi-day cold-air pools in a mountain valley. *Atmos. Environ.* **2012**, *46*, 17−24.

(52) Baasandorj, M.; Hoch, S. W.; Bares, R.; Lin, J. C.; Brown, S. S.; Millet, D. B.; Martin, R.; Kelly, K.; Zarzana, K. J.; Whiteman, C. D.; Dube, W. P.; Tonnesen, G.; Jaramillo, I. C.; Sohl, J. Coupling between chemical and meteorological processes under persistent cold-air pool conditions: evolution of wintertime PM2.5 pollution events and N2O5 observations in Utah's Salt Lake Valley. *Environ. Sci. Technol.* **2017**, *51*, 5941−5950.

(53) Hoek, G.; Beelen, R.; de Hoogh, K.; Vienneau, D.; Gulliver, J.; Fischer, P.; Briggs, D. A review of land-use regression models to assess spatial variation of outdoor air pollution. *Atmos. Environ.* **2008**, *42*, 7561−7578.

(54) Hasenfratz, D.; Saukh, O.; Walser, C.; Hueglin, C.; Fierz, M.; Thiele, L. In *Pushing the Spatio-Temporal Resolution Limit of Urban Air Pollution Maps*, 2014 IEEE International Conference on Pervasive Computing and Communications (PerCom); IEEE, 2014; pp 69−77.

(55) Lim, C. C.; Kim, H.; Vilcassim, M. J. R.; Thurston, G. D.; Gordon, T.; Chen, L.-C.; Lee, K.; Heimbinder, M.; Kim, S.-Y. Mapping urban air quality using mobile sampling with low-cost sensors and machine learning in Seoul, South Korea. *Environ. Int.* **2019**, *131*, No. 105022.

(56) Fritz, S.; See, L.; Carlson, T.; Haklay, M. M.; Oliver, J. L.; Fraisl, D.; Mondardini, R.; Brocklehurst, M.; Shanley, L. A.; Schade, S. *The Sustainable Development Goals Report 2019*; United Nations: New Yotk, 2019; 2.

(57) Li, J.; Zhang, H.; Chao, C.-Y.; Chien, C.-H.; Wu, C.-Y.; Luo, C. H.; Chen, L.-J.; Biswas, P. Integrating low-cost air quality sensor networks with fixed and satellite monitoring systems to study ground-level PM2.5. *Atmos. Environ.* **2020**, *223*, No. 117293.

(58) Ottosen, T.-B.; Kumar, P. Outlier detection and gap filling methodologies for low-cost air quality measurements. *Environ. Sci. Process. Impacts* **2019**, *21*, 701−713.

(59) Chen, L.; Ho, Y.; Hsieh, H.; Huang, S.; H, L.; Mahajan, S. ADF: An Anomaly Detection Framework for Large-Scale PM2.5 Sensing Systems. *IEEE Internet Things J.* **2018**, *5*, 559−570.

(60) Becnel, T.; Le, K.; Butterfield, A. E.; Kelly, K. E.; Giallardon, P. E. In *A Recursive Approach to Partially Blind Calibration of a Pollution Sensor Network*, 2019 IEEE International Conference on Embedded Software and Systems (ICESS); IEEE, 2019.

(61) Miskell, G.; Salmond, J.; Williams, D. E. Low-cost sensors and crowd-sourced data: Observations of siting impacts on a network of air-quality instruments. *Sci. Total Environ.* **2017**, *575*, 1119−1129.

https://dx.doi.org/10.1021/acs.est.0c02341
Environ. Sci. Technol. XXXX, XXX, XXX−XXX